with RNase A and then with RNase inhibitor (Table 4, item b). Purified RNA alone did not increase phage production (Table 4, item c). However, the inactive RNA-free proheads and the purified prohead RNA can be reconstructed, resulting in phage production (Table 4, item d), albeit at a relatively low efficiency compared to complementations of normal extracts and proheads (Tables 1 and 2). It is not clear whether this lower efficiency of assembly is due to alteration of the extracts with RNase and RNase inhibitor treatment or the quality of the purified RNA or RNA-free proheads.

In conclusion, we have demonstrated that a small RNA transcript of about 120 nucleotides from the far left end of the ϕ29 genome was a component of the ϕ29 prohead and that it had an essential role in ϕ29 DNA packaging in vitro. Some data have been obtained for systematic investigations of the possible role or roles of the small RNA in the initiation events of DNA-gp3 packaging (*11*) and the formation of the prohead-dependent and DNA-gp3–dependent ATPase (*12*) (as mentioned earlier). Treated proheads do not produce the aggregated forms of DNA-gp3 (Fig. 1), which are correlated with packaging efficiency (*11*), suggesting that an initiation step in DNA-gp3 packaging is blocked.

REFERENCES AND NOTES

1. T. C. King, R. Sirdeskmukh, D. Schlessinger, *Microbiol. Rev.* **50**, 428 (1986).
2. D. B. Bourgaize and M. J. Fournier, *Nature (London)* **325**, 281 (1987).
3. S. Casjens, in *Virus Structure and Assembly*, S. Casjens, Ed. (Jones and Bartlett, Portola Valley, CA, 1985), pp. 75–147.
4. M. A. Bjornsti *et al.*, *Proc. Natl. Acad. Sci. U.S.A.* **78**, 5861 (1981).
5. ———, *J. Virol.* **41**, 508 (1982).
6. ———, *ibid.* **45**, 383 (1983).
7. ———, *ibid.* **50**, 766 (1984).
8. ———, *ibid.* **53**, 858 (1985).
9. P. Guo, S. Grimes, D. Anderson, *Proc. Natl. Acad. Sci. U.S.A.* **83**, 3505 (1986).
10. M. Salas, *Current Topics Microbiol. Immunol.* **109**, 89 (1983).
11. P. Guo, C. Peterson, D. Anderson, *J. Mol. Biol.*, in press.
12. ———, *ibid.*, in press.
13. R. Gope and P. Serwer, *J. Virol.* **47**, 96 (1983).
14. P. Argos and J. E. Johnson, in *Biological Macromolecules and Assemblies, 1: Virus Structure*, F. A. Jurnak, A. McPherson, Eds. (Wiley, New York, 1984), pp. 1–43.
15. J. L. Carrascosa *et al.*, *J. Mol. Biol.* **154**, 311 (1982).
16. A. E. Sippel, *Eur. J. Biochem.* **37**, 31 (1973).
17. J. Ito, *J. Virol.* **28**, 895 (1978).
18. H. Yoshikawa and J. Ito, *Gene* **17**, 323 (1982).
19. J. M. Sogo *et al.*, *J. Mol. Biol.* **127**, 411 (1979).
20. I. Barthelemy, M. Salas, R. P. Mellado, *J. Virol.* **60**, 874 (1986).
21. D. J. Loskutoff and J. J. Pene, *ibid.* **11**, 87 (1973).

22. We thank C. Peterson, M. A. Gomes, and L. Lu for technical assistance; C. Church for typing the manuscript; and N. Anderson for the drawings of Fig. 3, A and B. Supported by NIH grant DE-3606.

9 February 1987; accepted 10 April 1987

Bacterial Resistance to β-Lactam Antibiotics: Crystal Structure of β-Lactamase from *Staphylococcus aureus* PC1 at 2.5 Å Resolution

OSNAT HERZBERG AND JOHN MOULT

β-lactamases are enzymes that protect bacteria from the lethal effects of β-lactam antibiotics, and are therefore of considerable clinical importance. The crystal structure of β-lactamase from the Gram-positive bacterium *Staphylococcus aureus* PC1 has been determined at 2.5 angstrom resolution. It reveals a molecule of novel topology, made up of two closely associated domains. The active site is located at the interface between the domains, with the key catalytic residue Ser^{70} at the amino terminus of a buried helix. Examination of the disposition of the functionally important residues within the active site depression leads to a model for the binding of a substrate and a functional analogy to the serine proteases. The unusual topology of the secondary structure units is relevant to questions concerning the evolutionary relation to the β-lactam target enzymes of the bacterial cell wall.

MANY TYPES OF DEFENSE MECHANISMS EXIST IN THE biological world, and relatively lowly life forms often exhibit a surprising degree of sophistication in these matters. One such system that has been used to advantage by man is the defense that some fungi mount, through the production of β-lactam antibiotics, against bacterial attack. These compounds kill bacterial cells by irreversibly inhibiting a number of enzymes concerned with cell wall synthesis and repair (*1*). A degree of complexity is added by the ability of some bacteria to defeat this fungal defense mechanism, primarily through the production of membrane-bound and excreted enzymes which hydrolyze β-lactam rings. These enzymes are known as β-lactamases or penicillinases (E.C. 3.5.2.6) (*2*). A variety of β-lactams are produced by fungi, and in turn, there are at least three different classes of β-lactamases produced by bacteria (*3*). A further layer of complexity is provided by the production of inhibitors of β-lactamases by some fungi (*4*).

The authors are members of the Medical Research Council of Canada Group in Protein Structure and Function, Department of Biochemistry, University of Alberta, Edmonton, Canada, T6G 2H7.

The β-lactam antibiotics have been in use for human and animal therapy for about 40 years. During that period, the ability to produce β-lactamases has become widespread amongst the pathogenic bacteria, primarily through the mechanism of plasmid exchange (*5*). As a result, the usefulness of the first generation of β-lactam antibiotics has been considerably reduced. A detailed knowledge of β-lactamase structures should facilitate the design of β-lactam antibiotics that will bypass this defense mechanism. Some compounds partially effective in this manner have been devised without knowledge of the relevant protein structures (*1, 6*). Alternatively, in vivo inhibitors of β-lactamases may be developed for use in a synergistic manner with the first generation β-lactam antibiotics. A naturally occurring inhibitor, clavulanic acid (*7*), is already in clinical use.

Amino acid sequence data of β-lactamases suggest three classes of these enzymes. This article is concerned with the class A enzymes, which involve an active site serine residue (*8*), but have no sequence relation to any known serine proteases. In contrast to the serine proteases, which utilize a histidine in the catalytic mechanism (*9*), class A β-lactamases lack a conserved histidine residue among the known sequences.

Class A enzymes show weak sequence homology to the cell wall penicillin-binding protein D-alanyl-D-alanine peptidase that participates in the synthesis of peptide crosslinks between polysaccharide chains structures (*1, 10*). Attention has also been drawn to the close structural analogy between the peptide links operated on by the cell wall enzymes and the β-lactam nucleus (*11, 12*). Thus, there has been speculation that β-lactamases evolved from the cell wall enzymes (*11*).

Class A β-lactamases exhibit an unusual flexibility. Some β-lactams reduce the catalytic efficiency of the enzymes, with a slow recovery to full activity, which can be aided by the presence of antibodies to the native structure (*13*). The flexibility may be related to an overall low stabilization (*14*), and to the existence of stable folding intermediates under denaturing conditions (*15*).

Crystallographic studies (*16*) on four class A enzymes are well advanced: from *S. aureus* (*16*, and this article), and from *Bacillus licheniformis* 749/C (*17*), *Bacillus cereus* 569 (*18*), and *Escherichia coli* R-TEM (*19*). Crystals have been reported for a class B (zinc requiring) β-lactamase (*18*), and for a class C β-lactamase (*20*). The structure of a cell wall penicillin-sensitive D-alanyl-D-alanine-peptidase has been published (*21*), as well as that of a penicillin-resistant Zn^{2+} containing peptidase (*22*). Comparisons of the penicillin-sensitive peptidase with the preliminary results for two of the class A β-lactamases (*17, 18*) point to structural similarities, supporting the suggestion of a possible evolutionary relationship. A more definitive evaluation of this relationship is now possible with the *S. aureus* β-lactamase structure, the first for which a complete polypeptide chain tracing is available.

We present here the structure of the extracellular class A β-lactamase from *S. aureus* PC1 at 2.5 Å resolution. The structure is sufficiently reliable to enable us to describe it in atomic detail. Examination of the disposition of the catalytically important residues reveals a relation to the serine proteases and leads to a model of the mode of binding of β-lactams. The probable cause of the activity related conformational flexibility is also explained. Thus, the way is open to the understanding of substrate specificity and to new drug design.

Structure determination. The structure determination followed the established procedures of protein crystallography, but the use of recent developments concerning crystallization technique and phase improvement was crucial.

The original crystals of β-lactamase from *S. aureus* PC1 were obtained in 1970 and, until recently, could not be reproduced. A 5 Å structure was determined from these crystals (*16*). We are now able to obtain large crystals through systematically modifying the

Table 1. Statistics for the structure determination of β-lactamase: heavy atom derivatives and refinement; rms, root mean square.

Heavy atom	Soaking time	Resolution	No. of unique reflections used	R_{iso}*	No. of sites	R_{cen}*	$\langle E_H \rangle / \langle f_H \rangle$*
2.5 m*M* $(C_2H_5HgO)_3PO$	3 days	3 Å	7109	0.244	1	0.61	0.69
1 m*M* $(NH_4)_2Pt(CN)_4$	23 days	3 Å	7154	0.146	2	0.69	0.84
1.5 m*M* $KAu(CN)_2$	6 days	3 Å	7162	0.095	3	0.71	1.05
			Refinement at 2.5Å				
$R(=\Sigma\|\|F_0\|-\|F_c\|\|/\Sigma\|F_0\|)$				0.284			
No. of reflections (6.0 to 2.5 Å)				9465 (>2σ)			
No. of atoms				2028			
Solvent				0			
No. of variable parameters (including individual B factors)				8113			
Average $\|F_0\|$				583 e			
Average $\|\|F_0\|-\|F_c\|\|$				166 e			
Average B factor				19.2 Å^2			
rms deviation bond distance				0.027 (0.030)†			
rms deviation bond angle distance				0.056 (0.040)			
rms deviation from planar group				0.046 (0.040)			
rms deviation from trans peptide				3.5° (4.0)			

$$* R_{iso} = \frac{\Sigma_h \| |F_{PH}obs| - |F_Pobs| \|}{\Sigma_h |F_Pobs|}$$

$$R_{cen} = \frac{\Sigma_{h\ centric} \| |F_{PH}obs| - |F_Pobs + F_Hcalc| \|}{\Sigma_h \| |F_{PH}obs| - |F_Pobs| \|}$$

$\langle E_H \rangle$, rms lack of closure error; $\langle f_H \rangle$ rms heavy atom scattering.
†The numbers in parentheses represent the values to which these parameters were restrained.

original crystallization conditions. In addition to the 78 percent saturated ammonium sulfate solution, we add 0.3*M* KCl, and also add small amounts of organic solvent. The solution is buffered at *p*H 8.0 with 100 m*M* NH_4HCO_3. The addition of organic solvents to salt solutions of proteins often improves crystal size and quality (*23*). A detailed study of this phenomenon has been published (*24*). In some cases impurities in polyethylene glycol (PEG) preparations may affect protein crystallization (*25*). In the case of β-lactamase, the presence of minute amounts of various organic solvents gives rise to crystals with varying morphology: ethanol, 2-methyl-2,4-penthanediol, PEG 200, and PEG 400 yield long thin needles; PEG 600 yields long thin plates. Large chunky crystals with two distinct morphologies are obtained in the presence of 0.3 to 0.6 percent (g/v) PEG 1000 and PEG 4000; precession photographs of crystals of these two types of crystals showed that they are isomorphous with the original crystals. They belong to space group *I*222, with unit cell dimensions $a = 54.36$ Å, $b = 93.69$ Å, $c = 138.70$ Å, and one protein molecule in the asymmetric unit. Crystals obtained from PEG 1000 solution were used for the structure determination.

Crystals were transferred to a solution of 90 percent saturated ammonium sulfate brought to *p*H ≃ 6 by the addition of NH_4HCO_3. X-ray intensity data to 3.0 Å resolution for the native and three heavy atom derivatives of low to mediocre quality were collected with an Enraf-Nonius CAD4 diffractometer; we followed a data collection protocol that has been described (*26*). Heavy atom binding sites were determined from difference Patterson maps and difference Fourier maps in the usual manner (*27*). The positional parameters and occupancies of the heavy atoms were refined by lack of closure error minimization (*28*). Some statistics for the heavy atom derivatives are given in Table 1. The multiple isomorphous replacement (MIR) method yielded a phase set with a figure of merit of 0.59. A 3 Å resolution electron density map was computed with the use of the centroid phases (*29*) and measured structure factor amplitudes weighted by the figure of merit. This map was rather noisy, but the contrast between protein and solvent regions was apparent and some secondary structure features could be identified.

Since approximately 65 to 70 percent of the crystal volume is solvent, we were able to improve the MIR map substantially by solvent flattening (*30, 31*). The procedure was started from the MIR map. Solvent region was defined with the automatic masking procedure of Wang (*31*). In order to avoid spurious flattening of protein regions, the solvent content was specified for masking purposes as only 50 percent of the crystal volume. The original algorithm was modified to use the local averaged absolute value of the electron density of the map rather than the local average value (*32*). The molecular shape obtained by masking was similar to that seen in the 5 Å MIR map, demonstrating proper performance of the procedure. After each step of mask calculation, one cycle of map modification and map inversion was performed with the Wang program suite. The resulting phases were combined with the phases from the previous step (initially the MIR phases), a new map was

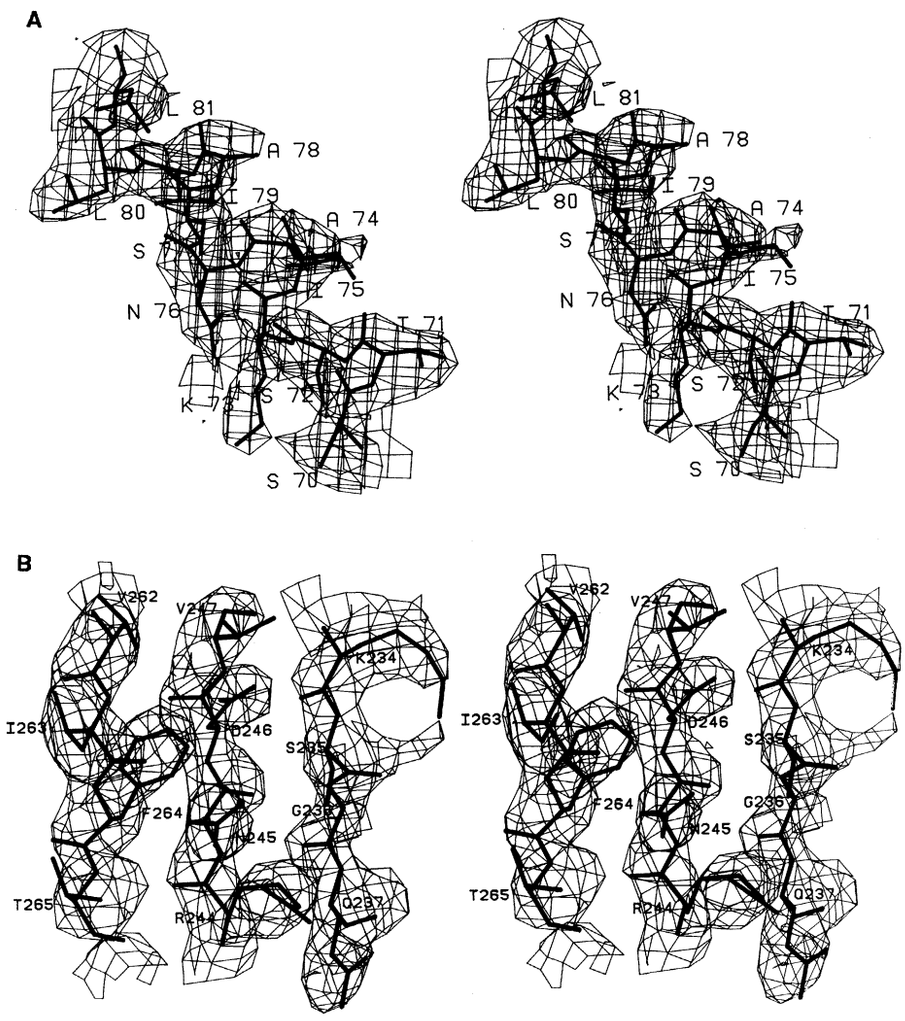

Fig. 1. Stereoscopic view of regions in the 3 Å resolution, solvent flattened, MIR electron density map. Superimposed on the map is the present 2.5 Å resolution polypeptide model. Labeling is according to Ambler's numbering scheme (*42*). The contour level is 0.25 e A^{-3} (**A**) The region for the central helix α2. Ser^{70} is the active site serine. (**B**) A portion of the antiparallel β sheet. Shown are four residues of each of strands (left to right) β5, β4, β3 (secondary structure assignment is given in the legend to Fig. 2). A segment of strand β3 (Lys^{234}–Ile^{239}) contributes to the substrate binding site. Single-letter abbreviations for the amino acid residues are: A, Ala; C, Cys; D, Asp; E, Glu; F, Phe; G, Gly; H, His; I, Ile; K, Lys; L, Leu; M, Met; N, Asn; P, Pro; Q, Gln; R, Arg; S, Ser; T, Thr; V, Val; W, Trp; and Y, Tyr.

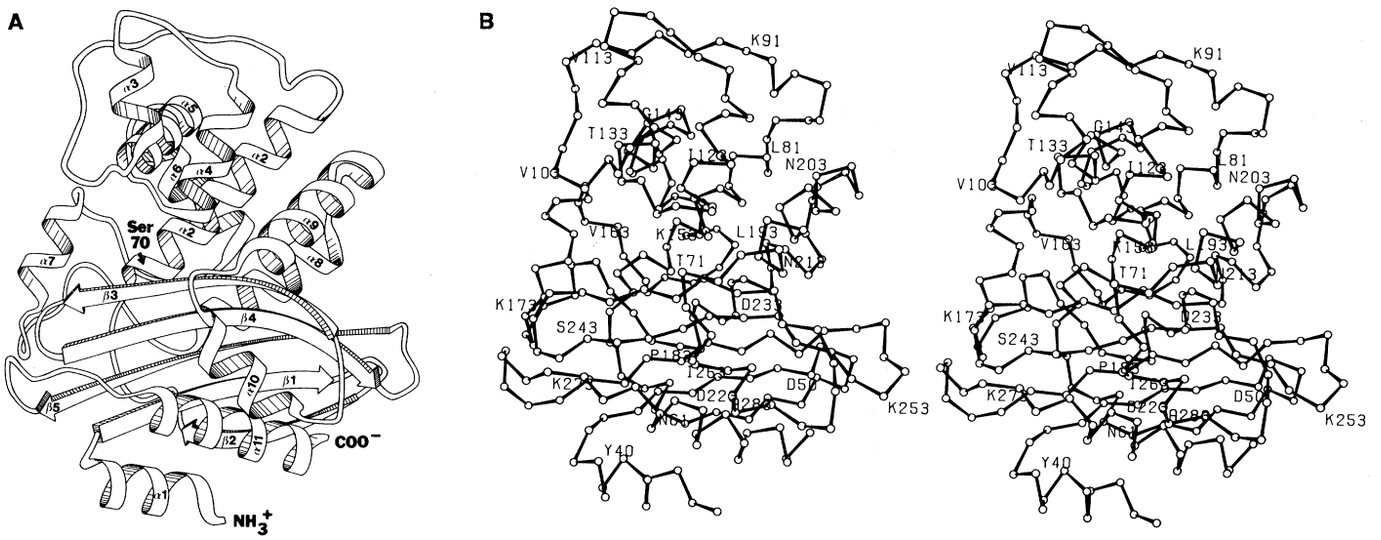

Fig. 2. The class A β-lactamase fold. (**A**) Ribbon representation of the polypeptide chain of β-lactamase from *S. aureus* PC1. Helices are labeled α and numbered sequentially through the amino acid sequence, strands are labeled β. The position for the active site serine Ser^{70} is shown. (**B**) Stereo representation showing the α-carbon positions in the molecule. Every fifth amino acid position is labeled according to Ambler (*42*). The exact residue for the start and end of secondary structure units may change after high resolution least squares refinement. The current assignments are: α1, 33–40; β1, 42–50; β2, 54–60; α2, 71–82; α3, 107–113; α4, 119–127; α5, 132–142; α6, 145–155; α7, 166–171; α8, 183–193; α9, 201–213; α10, 218–225; β3, 230–238; β4, 242–252; β5, 258–268; α11, 278–290. The large Ω-loop (*40*) near the active site includes residues 163–178.

calculated, and a new mask was produced. The mask was updated in this manner four times. This part of the protocol is similar to the reported work on glycolate oxidase (*33*). Finally, four cycles of map flattening and map inversion were performed with the fourth mask. The average cumulative phase shift from the initial MIR phases was 29.8°. The figure of merit was 0.81. This value should be considered as a measure of convergence and not an indication of the quality of the phases. However, the phase improvement was dramatically displayed in the resulting electron density map; its quality was far better than that of the original MIR map. Two typical examples of electron density in the final map are shown in Fig. 1.

A molecular model was fitted to the electron density map on the MMS-X graphics system (*34*), with the program M3. The polypeptide chain could be unambiguously traced, consistent with the known sequence (*35*). We extended the data to 2.5 Å resolution using a second native crystal. A preliminary restrained-parameter reciprocal space least-squares refinement (*36*) has been carried out with these data. The current R factor is 0.284 (see Table 1). The α-carbon coordinates have been deposited in the Brookhaven Protein Data Bank (*37*).

Molecular conformation of β-lactamase. The β-lactamase molecule forms an α + β protein (*38*) of novel topology (Fig. 2). The 257-residue long molecule may be considered to consist of two closely associated domains. One of these is formed by a five-stranded antiparallel beta sheet (with the topology: β2, β1, β5, β4, β3), and three helices (α1, α11, α10) that pack against one face of the sheet. The amino terminal and carboxyl terminal helices (α1, α11) are antiparallel, whereas the interhelix angle between α10 and α11 is about 45°. This arrangement is similar to an open-face β sandwich (*39*). However, in the case of β-lactamase there is no open face, since the second domain of the molecule packs against the second face of

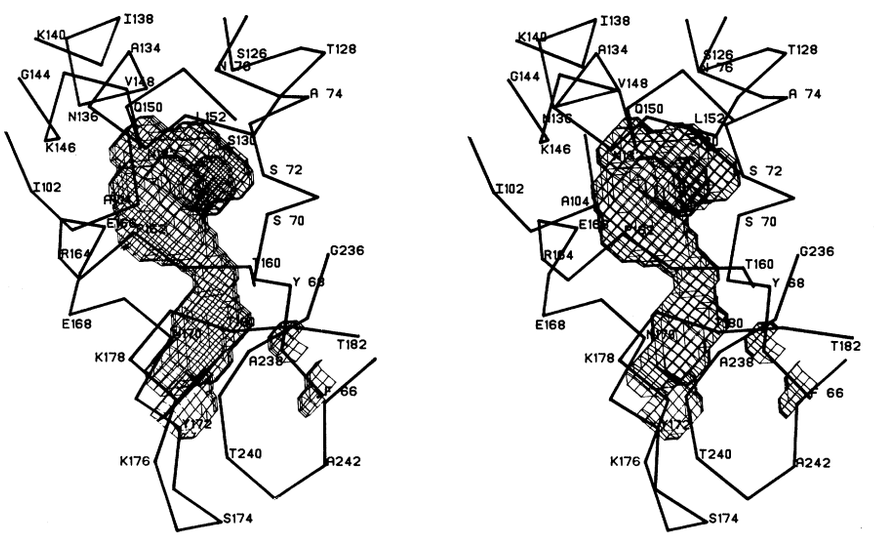

Fig. 3. A stereo plot of the large cavity in β-lactamase (the cave) displayed together with the α-carbon tracing of the polypeptide chain. In this view the buried active site helix α2 is seen on the right side of the figure. The Ω-loop (residues 163 to 178) is on the lower left side and helices α5 and α6 are at the top. The contours enclose the region of space accessible to some part of a 1.4 Å radius spherical probe. The radii of Chothia (*55*) were used to define solvent accessibility.

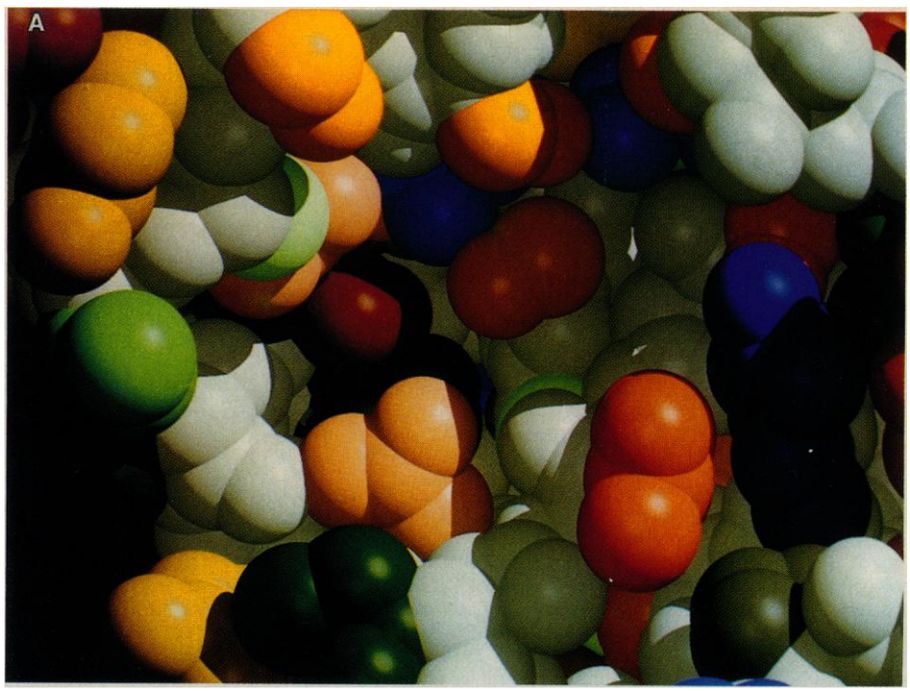

Fig. 4. Active site of β-lactamase from *S. aureus* PC1. (**A**) Computer-generated space filling model of the active site depression. Color scheme: white, main chain atoms; reds, negatively charged residues; blues, positively charged residues; greens, browns, gray, hydrophobic residues; oranges, pinks, polar residues. Ser^{70} can be seen in the center (orange), and the two lysines (blue), Lys^{73} and Lys^{234}, are nearby, as well as Glu^{166} (red). The picture was produced with the use of the program RASTER3D written by D. Bacon. (**B**) Stereoscopic view of the residues that make up the active site depression. The extent of the depression is demonstrated by contouring the solvent-accessible surface (accessibility defined as in the legend to Fig. 3). (**C**) As (B), with the proposed position of a bound ampicillin molecule. (**D**) The proposed conformation of ampicillin when bound to β-lactamase. Only the side chain conformation has been modified from that of the original crystal structure (*45*).

the sheet. The completely buried nature of the β sheet is unusual for an antiparallel structure, although very common for parallel sheets (*39*).

The second domain contains an arrangement of eight helices. The central helix (α2) is surrounded by five other helices (α4-α6, α8, α9), and two large surface loop structures. Each of these loops contains a short irregular helical segment (α3 and α7). The residue assignment for these two helices (legend to Fig. 2) may be revised after further refinement. The loop that contains helix α7 is 16 residues long and appears to be an omega loop (*40*).

Parts of helices α2, α7, α8, and α9 pack against the β sheet, but only α8 has an extensive contact region with the sheet face. Coverage of this face is also provided by an extended chain that connects strand β2 to helix α2, and runs across the sheet in a manner reminiscent of strands in β sandwiches.

The helical domain can be regarded as an insert between β2 and α10 of the sheet-containing domain. Thus, the sheet region is made from portions at the beginning and end of the polypeptide chain. The very long sheet crossover formed by the insertion of the helical domain and α10, between strands β2 and β3, is left-handed (*39*). A diagonal distance plot and a neighborhood correlation analysis (*41*) support the concept of a two-domain structure, although helices α8 and α9 are closely associated with both domains. There are two clefts in the structure, formed in the interface of the two domains, one of which is the active site depression. In the orientation of Fig. 2 the active site depression is on the left side of the molecule, and the second cleft is prominent on the right side.

Loose packing of β-lactamase. Analysis of internal cavities in β-lactamase, larger in volume than a water molecule, shows that the packing of this enzyme is strikingly imperfect. Two cavities are adjacent to the central helix α2, and are much too large to be an artifact of the incomplete refinement. One cavity is rather long and narrow (≃ 110 $Å^3$). The second (shown in Fig. 3) is an irregularly shaped cave whose limits are defined by helix α2, by the Ω-loop, and by residues on helices α5 and α6. A narrow exit to solvent is available from the side of the Ω-loop, around Tyr^{172} and Lys^{177} [we adopt the numbering scheme of Ambler (*42*), which is based on the alignment of four class A sequences]. A salt bridge between Lys^{73} and Glu^{166} blocks a possible opening to the active site depression (see next section). The cave volume is ≃330 $Å^3$, much larger than that usually observed in globular proteins for closed cavities (*43*). After the preliminary refinement there is an indication that part of this space is occupied by solvent. Such a loose packing suggests a possible conformational flexibility of the molecule between the Ω-loop and helix α2, which would affect the shape of the substrate binding site.

Three heavy atom compounds bind in the cave: the β-lactam hydrolysis product 6-(4-hydroxy-3,5-di-iodobenzamido)penicilloic acid, Pt-D-methionine (*16*), and ethyl mercury phosphate. The first two of these were expected to bind as substrate analogs, but the relative positions of their binding site and the active site serine are not compatible with substrate binding. We believe that these heavy atom compounds or some disintegration products from them bind in the cave without apparent relation to the catalytic activity.

Structure of the substrate binding site. Active site labeling experiments on several class A β-lactamases (*8*) all point to a serine residue at position 70 as the residue involved in the formation of an acyl enzyme intermediate with the carbonyl carbon of the β-lactam ring. Ser^{70} lies in one of two crevices across the enzyme surface formed at the interface of the helical domain with the β-sheet domain. When viewed from above, this crevice appears as a depression in the protein surface, with a floor approximately 17 by 7 Å, and a depth 6 Å below the surrounding protein surface (Fig. 4, A and B). Many of the amino acid residues in this area are conserved in four class A β-lactamase sequences (*42*). Toward the edge of the molecule, the depression narrows to a gully flanked by the side chains of Val^{103} and Ile^{239}. Val^{103} is a conserved residue, but Ile^{239} is an insertion in the *S. aureus* sequence with respect to those of the other class A β-lactamases. The side chain of Ser^{70} lies in the floor of the depression, and the ammonium group of Lys^{73}, another conserved residue, is immediately adjacent to it. The side chain of the conserved Glu^{166} also lies in the floor, and makes a salt bridge interaction with Lys^{73}. On the opposite side of the serine from Lys^{73}, the main chain NH groups of Ser^{70} and Gln^{237} point out of the surface. The side chain of a second conserved lysine residue, Lys^{234}, has its ammonium group in the wall at the closed end of the depression. These lysines have most of their side chains buried in the protein molecule. Movements about the last side chain dihedral

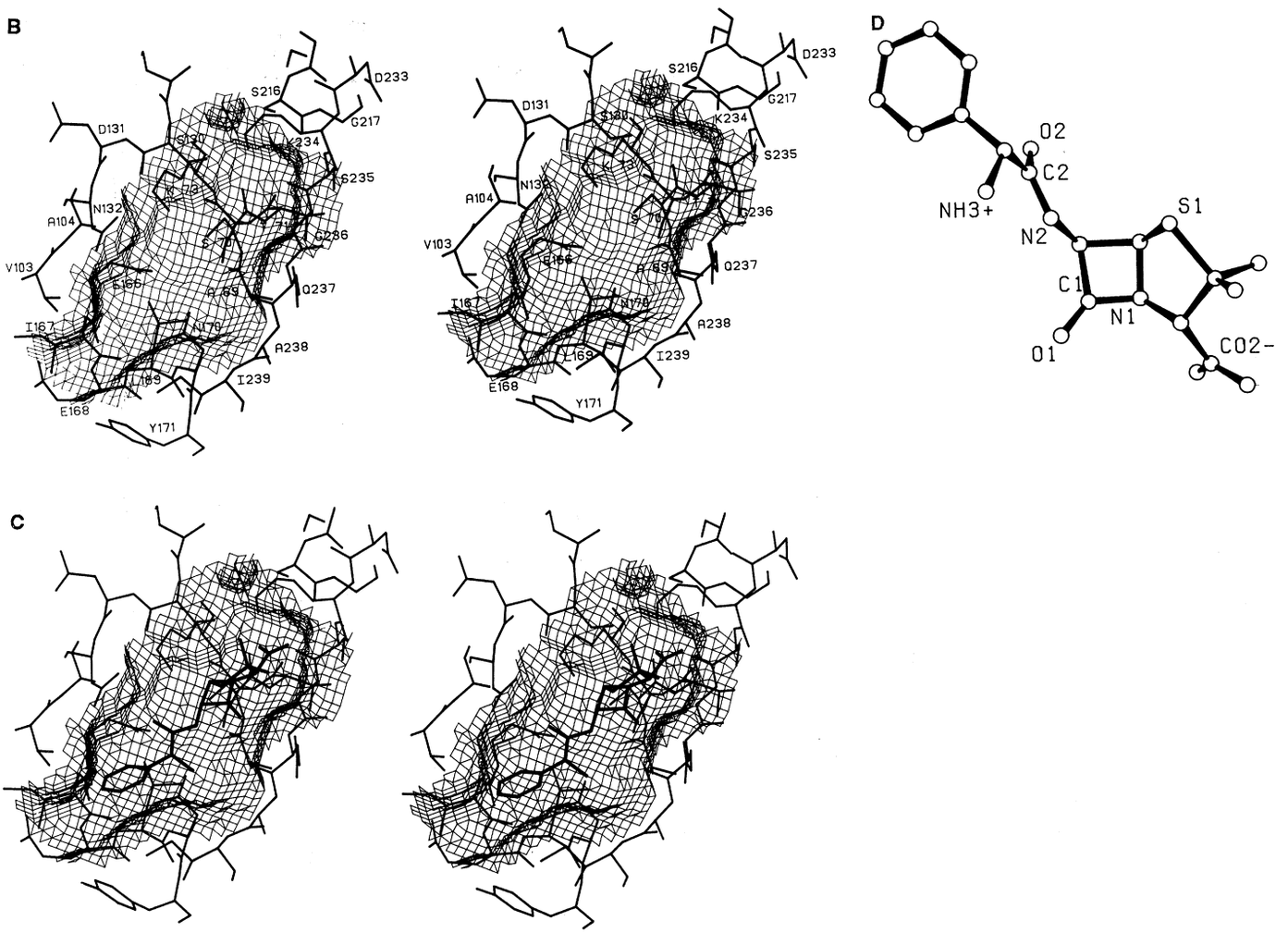

angle ($\chi 4$) are possible for both of them, though. Two conserved asparagine side chains, of residues 132 and 170, also lie in the walls of the depression, the first near to Glu^{166}, and the second near to Ile^{239}.

Ser^{70} is situated at the amino terminus of the buried central helix $\alpha 2$ of the helical domain, suggesting a role for the dipole of this helix in the catalytic mechanism (*44*). The large cavity in the structure adjacent to this helix (the cave) lies below the depression with its closest approach to the surface almost underneath Ser^{70}.

Proposed mode of binding of substrates. The size of the depression in the enzyme surface, the position of the catalytically important groups and other side chains, and the relatively rigid nature of β-lactam molecules suggest a mode of binding for the substrates. Model building was done exploiting the requirements of electrostatic, hydrophobic, and shape complementarity between enzyme and substrate. The resulting structure of the complex of the enzyme with the moderately good substrate ampicillin (*45*) (Fig. 4D) is shown in Fig. 4C. The following points were sufficient to determine the coordinates of the bound substrate, assuming no large-scale conformational changes of the protein:

1) The carbonyl-carbon atom (C1 in Fig. 4D) of the β-lactam ring must approach the Oγ of Ser^{70} in order to form the acyl enzyme.

2) The carboxyl group on the β-lactam five-membered ring, which is shielded from solvent as a consequence of point 1, must make appropriate electrostatic interactions with the protein. The only candidate for this interaction is the side chain ammonium group of the conserved Lys^{234}.

3) Points 1 and 2 determine the approximate position of the β-lactam nucleus with respect to the enzyme surface. Two different orientations of the fairly rigid β-lactam ring system are then possible. One of these places the carbonyl oxygen of the β-lactam ring over the side chain ammonium group of Lys^{73}, the other over the two exposed main chain amides of Ser^{70} and Gln^{237}. Both arrangements shield Lys^{73} and the NH groups from solvent in the complex, the former with the hydrogen bonding capacity of the main chain amides unsatisfied, making it unacceptable. In the second orientation, Lys^{73} makes no direct electrostatic interactions with the substrate but, because of its salt bridge with Glu^{166}, has an acceptable environment, while the Ser^{70} and Gln^{237} NH moieties interact in a satisfactory manner with the β-lactam ring carbonyl oxygen.

4) The specificity profile shows a clear preference for substrates with stereochemically unhindered hydrophobic end groups on the side chain of the β-lactam (*46*). The only candidate for the required favorable hydrophobic interactions is the hydrophobic gully formed by the side chains of Val^{103} and Ile^{239}. Adjustment of the side chain conformation of ampicillin allows favorable interactions of the phenyl ring with these residues (Fig. 4C).

With the previous points satisfied, the peptide link of the β-lactam side chain makes hydrogen bonds between its carbonyl oxygen (O2 in Fig. 4D) and the side chain of Asn^{132}, and between its amide group (N2) and the main chain carbonyl group of Gln^{237}, a satisfactory electrostatic environment.

The positively charged ammonium group of the side chain of ampicillin is partly desolvated in this arrangement, but makes

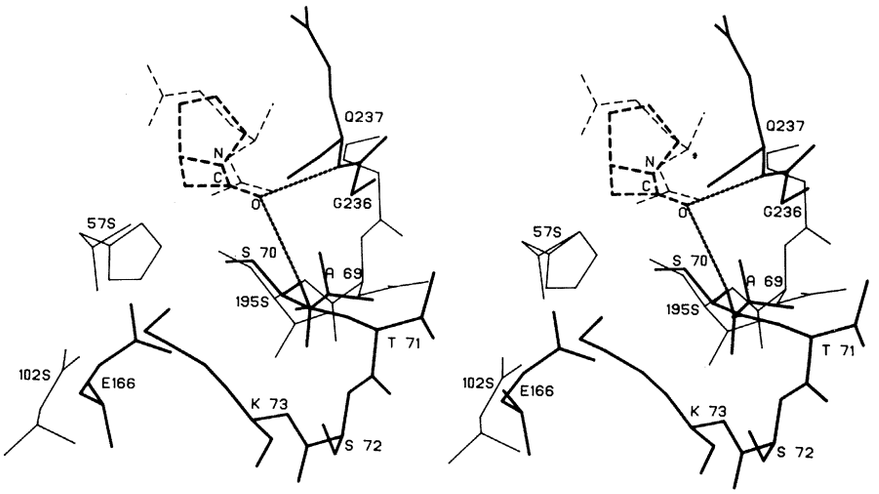

Fig. 5. A stereoscopic view of the superpositioning of the catalytically important residues of β-lactamase and the SGPB-ovomucoid inhibitor complex (*50*). β-Lactamase residues are shown in thick continuous lines and labeled according to Ambler (*42*). SGPB residues are in thin continuous lines, and the catalytic triad is labeled: 195S (Ser), 57S (His), 102S (Asp). A bound β-lactam nucleus is shown in thick dashed lines, and the equivalent peptide of the ovomucoid inhibitor (Leu^{18}, Glu^{19}) in thin dashed lines. The interaction between the β-lactam carbonyl oxygen and the amides of the oxyanion hole is shown in thick dotted lines.

electrostatic interactions with the side chain of Asn^{170} and the main chain carbonyl oxygen of Gln^{237}. These two charge-dipole interactions would appear to only partly offset the loss of solvation energy on binding. The situation is consistent with the observed K_m of this substrate being an order of magnitude lower than that of penicillin G, which differs only in the absence of the ammonium group. Such a mode of substrate binding is also consistent with the fact that β-lactams bearing more bulky and rigid side chains are fairly resistant to hydrolysis by class A β-lactamases (*46, 47*).

The complex has a short contact between the carboxyl group of the ampicillin five-membered ring and the main chain carbonyl oxygen of Ser^{235}. This contact is also elctrostatically unfavorable. A survey of the Cambridge Crystallographic Data Bank (*48*) shows that the β-lactam five-membered ring exhibits two different puckers with approximately equal frequency. It is possible that the one present in the crystal structure of ampicillin is not the optimum one for binding to the enzyme. More detailed model-building and high-resolution crystallographic binding studies of substrate analogs should clarify this point.

Comparison with the serine proteases. The use of a serine residue in the catalytic mechanism, the close relationship of the substrate molecule to a peptide, and the probable evolutionary relation of the class A β-lactamases to cell wall peptidases all suggest there are parallels with the well-studied serine proteases of the chymotrypsin and subtilisin families. These two structural classes of serine protease have very similar, although apparently evolutionarily independent, catalytic mechanisms (*9, 49*). Each has an active site serine, an adjacent histidine residue, and a buried aspartic acid interacting with the histidine. Two NH groups form hydrogen bonds to the carbonyl oxygen adjacent to the scissile bond of a substrate, creating an environment known as the oxyanion hole (*9*). In addition, a serine residue in the subtilisin family lies at the amino terminus of a buried α-helix, suggesting a role for the helix dipole in catalysis (*44*).

What are the equivalent arrangements in the class A β-lactamases? To assess this, we compared the structure of a complex of a chymotrypsin type serine protease—protease B from *Streptomyces griseus* (SGPB)—and a bound protein inhibitor (the third domain of the ovomucoid inhibitor from turkey) (*50*) with the *S. aureus* β-lactamase. The crystallographic coordinates of the relevant atoms of SGPB were superimposed on those of the β-lactamase by means of a least squares fit. These atoms are the α- and β-carbons of the active site serine residues (residue 70 in β-lactamase, 195 in SGPB) and the main chain nitrogens of the respective oxyanion holes. The root-mean-square discrepancy between the four atoms in the two structures after superposition is 0.3 Å.

The two aligned structures (Fig. 5) indicate that the ammonium group of Lys^{73} in β-lactamase falls close to the side chain of the catalytic His^{57} in SGPB. There is no analogous residue to the Asp^{102} of SGPB at the equivalent position in β-lactamase. However, Glu^{166} interacts with Lys^{73}, and is shielded from solvent in the presence of a substrate. The structure alignment also results in a similar spatial disposition of the respective substrates, with the equivalents of the scissile bond and its neighboring atoms closer than 1 Å.

The catalytic mechanism. The likely steps in the catalytic process are (*1*): (i) Formation of the acyl enzyme intermediate, via a tetrahedral transition state of the β-lactam carbonyl carbon and transfer of a proton from Ser^{70} to the β-lactam ring nitrogen. (ii) Hydrolysis of the acyl enzyme complex. Our model of substrate binding suggests how these steps are accomplished in the β-lactamases.

Stabilization of the tetrahedral transition state on the pathway to the acyl enzyme complex is provided by the interaction of the β-lactam carbonyl oxygen with the oxyanion hole and the dipole of the α2 helix, in a manner similar to that of the serine proteases, particularly subtilisin (*9, 44*).

Proton transfer from the serine to the β-lactam nitrogen is apparently facilitated by the presence of Lys^{73}. This residue cannot act as a temporary resting place for the proton, as has been postulated for the structurally equivalent histidine residue of the serine proteases, because of its high *p*K. However, Lys^{73} is positioned to orient the serine proton toward the nitrogen in the Michaelis complex, to provide a potential gradient which reduces the energy barrier for the proton transfer, and to polarize the nitrogen favorably to receive the proton.

These considerations do not apply so clearly to the case of the cell wall peptidases, where the reverse transfer of the proton would appear to be required for transpeptidation. Nevertheless, the lysine residue is conserved in those amino acid sequences. Interestingly, the kinetics of these enzymes is not straightforward. In particular, the initial peptide cleavage of a D-Ala-D-Ala sequence is irreversible (*51*).

We propose that Glu^{166} is involved in the deacylation step, which cannot be carried out in the same manner as in the serine proteases. There, departure of the leaving group is believed to allow the binding of a water molecule, so that deacylation takes place as the simple reversal of acylation, requiring no additional machinery. In contrast, the leaving group in the β-lactam acyl complex is covalently bonded through the remainder of the four-membered ring to the carbonyl carbon, making replacement by water impossible. Attack of a water molecule must therefore come from the opposite direction. Examination of the model of the enzyme substrate complex shows

that there is a nice site for a water molecule to bind in the appropriate position to perform this function. This site lies between the peptide bond of the β-lactam side chain and the enzyme surface, at the bottom of the depression, and has hydrogen bonding to the main chain carbonyl group of Gln^{237}, the side chain of Asn^{170}, and the carboxyl group of Glu^{166}. The latter interaction suggests that the role of the glutamate is to enhance the nucleophilic attack of the water molecule. It may be that the cell wall peptidases do not have such an optimized water binding site, resulting in very slow decay of the complex, and effective antibiotic action.

Suicide inhibitors of class A β-lactamases have been designed incorporating a proton with enhanced acidity at the side–chain bearing carbon of the β-lactam ring (*8*). It has been proposed (*52*) that this proton is abstracted by a base on the enzyme. In our model, Glu^{166} is properly oriented, although somewhat distant, to perform this role for a β conformation at this carbon. Further, the electrostatic interaction of the β-lactam carbonyl oxygen with the oxyanion hole would facilitate such a reaction.

Evolution of class A β-lactamases. Although there is sequence homology around the active site of class A β-lactamases and the D-alanyl-D-alanine peptidase (*1, 10*), the overall homology is low. The comparison of the preliminary crystallographic results for the class A β-lactamases (from *Bacillus licheniformis* 749/c and *Bacillus cereus* 569) shows a similar spatial disposition of some secondary structure units to that of the D-alanyl-D-alanine peptidase (*17, 18*). The division into two regions, one containing a β sheet and the other being predominantly helical, is common to all three of these enzymes and to the *S. aureus* β-lactamase. Chain continuity has not been determined for the two β-lactamases used for the comparisons, although the high degree of sequence homology makes it extremely likely that this must be identical to that of the *S. aureus* PC1. Reported chain continuity for the D-alanyl-D-alanine peptidase (*21*) is quite different from the *S. aureus* β-lactamase. For example, in β-lactamase the antiparallel β sheet and helices α1, α10, and α11 lying on one side of the sheet are formed by both amino terminal and carboxyl terminal parts of the sequence. In contrast, this region is reported to consist of a continuous central sequence in the penicillin target enzyme (residues 150 to 265). The antiparallel arrangement of the sheet in β-lactamase also differs from the sheet of the penicillin target enzyme, where three adjacent strands have been reported to be parallel. However, the catalytic arrangements are strikingly similar, with an active site serine at the amino terminus of a helix and a conserved lysine. This strongly suggests an evolutionary relationship. The polypeptide chain tracing of Kelly *et al.* was obtained prior to the determination of the amino acid sequence, and the 2.8 A resolution of electron density map was discontinuous in some regions (*21*). Thus, the topology may be revised and become more similar to that of β-lactamase.

The β-lactamase from *S. aureus* does not appear to be related to any other known protein structure. It has been suggested that the structure of β-lactamase may be evolutionarily related to that of lysozyme (*53*). Although the structure of *S. aureus* β-lactamase is reminiscent of that of T4 lysozyme, structure comparison by the procedure of Remington and Matthews (*54*) gives no support for this hypothesis.

REFERENCES AND NOTES

1. J. M. Frère and B. Joris, *CRC Crit. Rev. Microbiol.* **11**, 299 (1985).
2. E. P. Abraham and E. B. Chain, *Nature (London)* **146**, 837 (1940).
3. R. P. Ambler, *Philos. Trans. R. Soc. London Ser. B* **289**, 321 (1980); B. Jaurin, T. Grundstrom, *Proc. Natl. Acad. Sci. U.S.A.* **78**, 4897 (1981).
4. M. Cole, in *β-Lactamases*, J. M. T. Hamilton-Miller and J. T. Smith, Eds. (Academic Press, London, 1979), pp. 205–289.
5. R. B. Sykes and M. H. Richmond, *Nature (London)* **226**, 952 (1970).
6. J. M. T. Hamilton-Miller, in *β-Lactamases*, J. M. T. Hamilton-Miller and J. T. Smith, Eds. (Academic Press, London, 1979), pp. 1–16.
7. C. Reading, M. Cole, *Antimicrob. Agents Chemother.* **11**, 852 (1977).
8. V. Knott-Hunziker, S. G. Waley, B. S. Orlek, P. G. Sammes, *FEBS Lett.* **99**, 59 (1979); S. J. Cartwright, A. F. W. Coulson, *Philos. Trans. R. Soc. London Ser. B* **289**, 370 (1980); C. Kemal and J. R. Knowles, *Biochemistry* **20**, 3688 (1981).
9. J. Kraut, *Annu. Rev. Biochem.* **46**, 331 (1977).
10. D. J. Waxman and J. L. Strominger, *J. Biol. Chem.* **255**, 3964 (1980).
11. D. J. Tipper and J. L. Strominger, *Proc. Natl. Acad. Sci. U.S.A.* **54**, 1133 (1965).
12. D. B. Boyd, *J. Med. Chem.* **22**, 533 (1979).
13. N. Citri, A. Samuni, N. Zyk, *Proc. Natl. Acad. Sci. U.S.A.* **73**, 1048 (1976); R. Virden, A. F. Bristow, R. H. Pain, *Biochem. Biophys. Res. Commun.* **82**, 951 (1978).
14. B. Robson and R. H. Pain, *Biochem. J.* **155**, 325 (1976).
15. E. A. Carrey and R. H. Pain, *Biochim. Biophys. Acta* **533**, 12 (1978); T. E. Creighton and R. H. Pain, *J. Mol. Biol.* **137**, 431 (1980).
16. J. Moult *et al.*, *Biochem. J.* **225**, 167 (1985).
17. J. A. Kelly *et al.*, *Science* **231**, 1429 (1986).
18. B. Samraoni *et al.*, *Nature (London)* **320**, 378 (1986).
19. M. L. DeLucia, J. A. Kelly, M. M. Mangion, P. C. Moews, J. R. Knox, *Philos. Trans. R. Soc. London Ser. B* **289**, 361 (1980).
20. P. Charlier, O. Dideberg, J. M. Frère, P. C. Moews, J. R. Knox, *J. Mol. Biol.* **171**, 237 (1983).
21. J. A. Kelly *et al.*, *J. Biol. Chem.* **260**, 6449 (1985).
22. O. Dideberg *et al.*, *Nature (London)* **299**, 469 (1982).
23. O. Herzberg, K. Hayakawa, M. N. G. James, *J. Mol. Biol.* **112**, 345 (1984); M. Fujinaga and M. N. G. James, *ibid.* in press.
24. W. J. Ray, Jr., and C. E. Bracker, *J. Cryst. Growth* **76**, 562 (1986).
25. F. Jurnak, *ibid.*, p. 577.
26. M. N. G. James, A. Sielecki, F. Salituro, D. H. Rich, T. Hofmann, *Proc. Natl. Acad. Sci. U.S.A.* **79**, 6137 (1982).
27. T. L. Blundell and L. N. Johnson, *Protein Crystallography* (Academic Press, London, 1976).
28. R. E. Dickerson, J. E. Weinzierl, R. A. Palmer, *Acta Cryst.* **B24**, 997 (1968).
29. D. M. Blow and F. H. C. Crick, *ibid.* **12**, 794 (1959).
30. R. W. Schevitz, A. D. Podjarny, M. Zwick, J. J. Hughes, P. B. Sigler, *ibid.* **A37**, 669 (1981).
31. B. C. Wang, *Methods Enzymol.* **115B**, 90 (1985).
32. W. F. Anderson and A. K. Muir, personal communication.
33. Y. Lindqvist and C.-I. Brändén, *Proc. Natl. Acad. Sci. U.S.A.* **82**, 6855 (1985).
34. A. R. Sielecki, M. N. G. James, C. G. Broughton, in *Crystallographic Computing, Proceedings of the International Summer School at Carleton University*, D. Sayre, Ed., (Oxford Univ. Press, Oxford, 1982), pp. 409–419.
35. R. P. Ambler, *Biochem. J.* **151**, 197 (1975).
36. W. A. Hendrickson and J. H. Konnert, in *Biomolecular Structure, Function, Conformation and Evolution*, R. Srinivasan, Ed. (Pergamon, Oxford, 1980), vol. 1, pp. 43–57.
37. F. C. Bernstein *et al.*, *J. Mol. Biol.* **112**, 535 (1977).
38. M. Levitt and C. Chothia, *Nature (London)* **261**, 552 (1976).
39. J. Richardson, *Adv. Protein Chemistry* **34**, 167 (1981).
40. J. F. Leszczynski and G. D. Rose, *Science* **234**, 849 (1986).
41. G. E. Schultz and R. H. Schirmer, *Principles of Protein Structure* (Springer-Verlag, New York, 1979).
42. R. P. Ambler, in *β-Lactamases*, J. M. T. Hamilton-Miller and J. T. Smith, Eds. (Academic Press, New York, 1979), pp. 99–125.
43. A. A. Rashin, M. Iofin, B. Honig, *Biochemistry* **25**, 3619 (1986).
44. W. G. J. Hol, in *Prog. Biophys. Mol. Biol.* **45**, 149 (1985).
45. M. N. G. James, D. Hall, D. C. Hodgkin, *Nature (London)* **220**, 168 (1968).
46. R. H. Depue, A. G. Moat, A. Bondi, *Arch. Biochem. Biophys.* **107**, 374 (1964); M. H. Richmond, *Biochem. J.* **88**, 452 (1963); **94**, 584 (1965).
47. J. P. Hou and J. W. Poole, *J. Pharm. Sci.* **60**, 503 (1971).
48. F. H. Allen *et al.*, *Acta Cryst.* **B35**, 2331 (1979).
49. J. D. Robertus, J. Kraut, R. A. Alden, J. J. Birktoft, *Biochemistry* **11**, 4293 (1972).
50. M. Fujinaga *et al.*, *Proc. Natl. Acad. Sci. U.S.A.* **79**, 4868 (1982).
51. J. M. Frère, J. M. Ghuysen, H. R. Perkins, M. Nieto, *Biochem. J.* **135**, 483 (1973).
52. R. L. Charnas, J. Fisher, J. R. Knowles, *Biochemistry* **17**, 2185 (1978).
53. M. R. Pollock, *Proc. R. Soc. London Ser. B* **179**, 385 (1971).
54. S. J. Remington and B. W. Matthews, *Proc. Natl. Acad. Sci. U.S.A.* **75**, 2180 (1978).
55. C. Chothia, *J. Mol. Biol.* **105**, 1 (1976).

56. Most of this work was carried out in the laboratory of M. N. G. James. We thank him for his support, encouragement, and wisdom. We also thank A. Sielecki and W. Anderson for helpful discussions; D. Bacon for computer programs for structure comparison and color graphics; B. C. Wang for the solvent flattening program suite; K. Hayakawa for all we learned form her about crystallization; and A. Yonath and J. Sussman for suppport during our work in the Weizmann Institute of Science; A. Coulson for providing facilities at the University of Edinburgh for the enzyme preparation; and R. Ambler and L. Sawyer for the provision of facilities and for help and encouragement. Supported by a grant from the Medical Research Council of Canada to the Group in Protein Structure and Function at the University of Alberta, by an Alberta Heritage Foundation for Medical Research fellowship award (O.H.), by an Alberta Heritage Foundation for Medical Research visiting scientist award (J.M.), and by an EMBO short-term fellowship (J.M.).

24 February 1987; accepted 15 April 1987